

# Dislocation Mechanisms in the GaN Lateral Overgrowth by Hydride Vapor Phase Epitaxy

T. S. Kuan, C. K. Inoki, Y. Hsu, and D. L. Harris

Department of Physics, University at Albany, State University of New York, Albany, NY 12222

R. Zhang, S. Gu, and T. F. Kuech

Department of Chemical Engineering, University of Wisconsin, Madison, WI 53706

## ABSTRACT

We have carried out a series of lateral epitaxial overgrowths (LEO) of GaN through thin oxide windows by the hydride vapor phase epitaxy (HVPE) technique at different growth temperatures. High lateral growth rate at 1100°C allows coalescing of neighboring islands into a continuous and flat film, while the lower lateral growth rate at 1050°C produces triangular-shaped ridges over the growth windows. In either case, threading dislocations bend into laterally grown regions to relax the shear stress developed in the film during growth. In regions close to the mask edge, where the shear stress is highest, dislocations interact and multiply into arrays of edge dislocations lying parallel to the growth window. This multiplication and pileup of dislocations cause a large-angle tilting of the laterally grown regions. The tilt angle is high (~8 degrees) when the growth is at 1050°C and becomes smaller (3-5 degrees) at 1100°C. At the coalescence of growth facets, a tilt-type grain boundary is formed. During the high-temperature lateral growth, the tensile stress in the GaN seed layer and the thermal stress from the mask layer both contribute to a high shear stress at the growth facets. Finite element stress simulations suggest that this shear stress may be sufficient to cause the observed excessive dislocation activities and tilting of LEO regions at high growth temperatures.

## INTRODUCTION

The lateral epitaxial overgrowth (LEO) technique has recently been explored as a promising approach to reduce the dislocation density in GaN layers grown on a substrate. Various degrees of success using this method have been reported [1-4]. In GaN lateral overgrowth experiments using metalorganic vapor phase epitaxy (MOVPE) at 1000-1100°C, the dislocations originated from the seed layer are confined mostly over the growth windows [1, 2]. In a GaN lateral growth over a thin SiO<sub>2</sub> mask at 1000°C by hydride vapor-phase epitaxy (HVPE), however, most dislocations bend laterally into the overgrown regions [3, 4]. In either case, the defect density in the overgrown layer is reduced, since only the portion of defects in the seed layer not masked by the thin SiO<sub>2</sub> layer is able to propagate into the upper layer. During the LEO by either MOVPE or HVPE growth technique, arrays of edge dislocations are introduced at the mask edges, and they collectively tilt the c-axis of the LEO regions away from the [0001] epitaxial direction [2, 4]. The observed tilt ranges from less than ~0.2° [2] to larger than 10°. The correlation of c-axis tilt to growth technique and condition has not been established. In this study, we have carried out a series of LEO experiments and finite element stress simulations aimed at understanding the cause of LEO tilt and the associated dislocation mechanisms.

## EXPERIMENTAL

The substrates used for our LEO experiments were 2.7- $\mu\text{m}$ -thick GaN seed layers grown by MOVPE on a sapphire substrate. A 0.2- $\mu\text{m}$ -thick  $\text{SiO}_2$  mask layer was grown on top by tetraethoxysilane (TEOS)-based chemical vapor deposition at  $\sim 600^\circ\text{C}$ , and growth windows were patterned by standard optical lithography and etching processes. The pattern consisted of 3- or 4- $\mu\text{m}$ -wide stripe openings parallel to the  $[1\bar{1}00]$  direction separated by 8- $\mu\text{m}$ -wide mask areas. In one sample (sample no. 3), the stripes (5.5  $\mu\text{m}$  in width) were arranged in a radial pattern, allowing comparisons to be made between the LEO process along different lateral growth directions.

The samples were grown in a vertical HVPE reactor [5]. The samples were introduced into the growth region of the system under flowing  $\text{NH}_3$  and  $\text{N}_2$ . The growth was initiated by the introduction of HCl to the Ga source region. The sample was kept at a constant temperature and gas phase ambient during growth. The five growth conditions investigated are listed in Table 1. Many factors influence the growth of HVPE GaN. We have altered the growth temperature in this study since it is the primary variable affecting the growth behavior.

**Table 1** Growth conditions, growth rate, and defect structure

Sample	$T_g$ ( $^\circ\text{C}$ )	$\text{NH}_3$ flow rate (sccm)	HCl flow rate (sccm)	Vertical growth rate ( $\mu\text{m}/\text{h}$ )	Lateral growth rate ( $\mu\text{m}/\text{h}$ )	c-axis tilt
1	1050	600	18	8	3.6	$7^\circ$
2	1050	1000	18	13	6	$8^\circ$
3a	1075	1000	22.5	24	14	$8^\circ$
3b	1075	1000	22.5	24	2.4	$10^\circ$
4	1100	600	18	9.6	20	$3^\circ$
5	1100	1000	18	5.8	20	$5^\circ$

## RESULTS AND DISCUSSION

### A. Growth morphology

Triangular-shaped ridge growth was observed at  $1050^\circ\text{C}$  over 3- $\mu\text{m}$ -wide stripe openings parallel to the  $[1\bar{1}00]$  direction in sample no. 1 [Fig. 1(a)]. The growth facets are curved before coalescing into a continuous film. In sample no. 2, higher  $\text{NH}_3$  flux (1000 sccm) results in higher growth rate. The lateral/vertical growth rate ratio ( $= 0.45$ ) and the ridge growth morphology remain the same as in sample no. 1, but coalescing has occurred, and the film has become continuous.

In sample no. 3a, higher ( $\sim 2\times$ ) lateral and vertical growth rates with a lateral/vertical rate ratio of about 0.6 were observed on stripe windows parallel to the  $[1\bar{1}00]$  direction. The increase in growth rate is mostly due to the higher HCl flow rate. In sample no. 3b, the stripe windows are parallel to the  $[1\bar{1}\bar{2}0]$  direction, and the lateral growth rate is much smaller (2.4  $\mu\text{m}/\text{hr}$ ), resulting in a lateral/vertical rate ratio of  $\sim 0.1$ . From the scanning electron microscope images, we learned that on  $[1\bar{1}\bar{2}0]$ -oriented windows, the LEO is on  $(\bar{1}101)$  and  $(1\bar{1}01)$  facets, while on  $[1\bar{1}00]$ -oriented windows, the growth is on  $(11\bar{2}2)$  and  $(\bar{1}\bar{1}22)$  facets. Our observations imply a much slower LEO rate on  $(\bar{1}101)$  and  $(1\bar{1}01)$  facets. Similarly strong dependencies of growth rate on facet

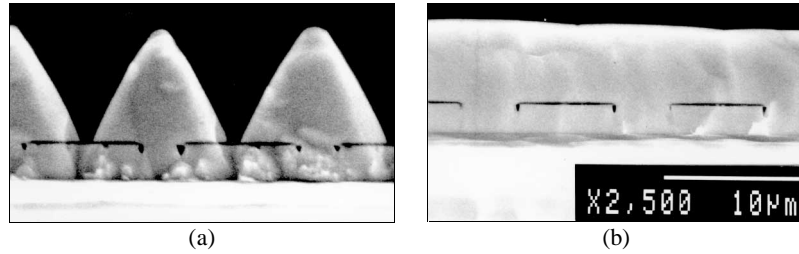


**Fig. 1** Cross-sectional SEM images of GaN grown on windows parallel to the  $[1\bar{1}00]$  direction: (a) sample no. 1 grown for one hour. (b) sample no. 5 grown for one hour.

plane have also been reported for the lateral growth of GaN by MOVPE [1]. In samples no. 4 and no. 5, coalesced and smooth films were grown over parallel,  $[1\bar{1}00]$ -oriented windows at  $1100^\circ\text{C}$  [Fig. 1(b)]. The lateral growth rate at this temperature is estimated to be at least  $20\ \mu\text{m/h}$  from the film's surface curvature directly above the growth window.

### B. Dislocation structure

Some morphological features such as the curved LEO facets observed in Fig. 1(a) can be attributed to the dislocation mechanisms involved during the growth. A cross-sectional TEM image of sample no. 1 in Fig. 2(a) reveals the dislocation structure after the sample is cooled to room temperature. A triangular ridge structure (region A) is grown first before the LEO occurs. This ridge structure contains vertical threading dislocations, mostly edge type with  $b = 1/3\langle 11\bar{2}0 \rangle$ , propagating from the MOVPE seed layer [3, 6]. This initial structure has two facets extending at  $66^\circ$  from the edges of the growth window, as marked by the dashed lines in Fig. 2(b). Since no low-index atomic planes parallel to  $[1\bar{1}00]$  are inclined at  $66^\circ$  from the (0001) plane, the observed angle may be determined by the lateral/vertical growth ratio [Table 1,  $\tan^{-1}(8/3.6) = 66^\circ$ ]. As LEO proceeds from the two ridge surfaces, all dislocations bend toward the growth surfaces and propagate on horizontal (0001) planes and on inclined lattice planes such as (11 $\bar{2}$ 2), (11 $\bar{2}$ 3), and (11 $\bar{2}$ 4), leaving the region B directly above the growth windows

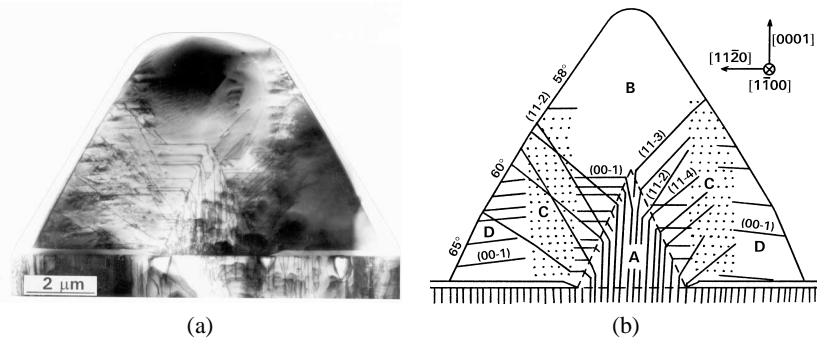


**Fig. 2** (a) A cross-sectional TEM image of a GaN ridge structure grown at  $1050^\circ\text{C}$  (sample no. 1). (b) Schematic of the dislocation glide behavior and final configuration in a GaN ridge structure observed in (a).

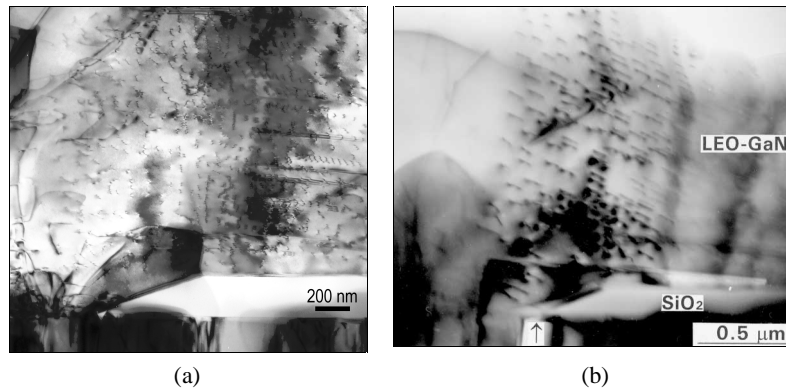
depleted of dislocations. The image force and/or the presence of shear stress close to the ridge surfaces may have caused the dislocation bending at high growth temperatures.

Fig. 2 indicates further that in LEO regions close to the mask edge (regions C), extensive dislocation multiplication has occurred, producing arrays of edge dislocations lying parallel to the  $[1\bar{1}00]$  ridge direction. These are perfect dislocations since no stacking fault contrast was observed on the slip planes. It is possible that the Frank-Reed type sources [7] are in operation for the generation of parallel dislocations during growth. These arrays of edge dislocations, confined mostly to the region C and constituting a series of tilt-type boundaries, tilt the  $c$ -axis of the crystal grown beyond region C away from the  $[0001]$  epitaxial orientation. A 7-degree  $c$ -axis tilt is measured from the image contrast of dislocations gliding on the tilted  $(0001)$  planes in region D in Fig. 2(a). As a result of the  $7^\circ$  tilt, the lower part of the  $(11\bar{2}2)$  facets on both sides of the ridge bends from the original  $58^\circ$  to a steeper  $65^\circ$  angle [Fig. 2(b)].

The crystal tilt remains in the rest of LEO films as growth continues, and, at the coalescence of growth facets, formation of a tilt-type grain boundary is unavoidable. The amount of crystal tilt can be measured accurately in a diffraction pattern taken from the bi-crystal at the coalescing boundary. The tilt angles measured for various growth conditions are listed in Table 1. In general, more parallel dislocations are observed in samples with higher tilt angles. Sample no. 3b has the largest  $c$ -axis tilt, and in it we find the highest density of edge dislocations in region C, as shown in Fig. 3(a). Fig. 3(b) shows the dislocation arrays observed near the  $\text{SiO}_2$  mask edge in the sample no. 5. These parallel dislocations line up vertically into a series of about 15 low-angle tilt boundaries. With a measured vertical dislocation spacing  $D$  of about 50 nm and  $b = 0.3$  nm, the tilt angle of each boundary is estimated to be  $\theta \sim b/D \sim 0.35^\circ$ . The total tilt accumulated by the  $\sim 15$  boundaries is about  $5^\circ$ , which is in good agreement with the diffraction measurement (Table 1).

### C. Shear stress in LEO structures

The dislocation bending and  $c$ -axis tilting are most prominent in HVPE growth. The higher growth rates in HVPE result in LEO islands of high aspect ratio and large exposed surface area when compared to MOVPE growth. Since dislocations are



**Fig. 3** TEM images of arrays of edge dislocation pileups parallel to the  $\text{SiO}_2$  mask edge: (a) sample no. 3b and (b) sample no. 5.

observed to glide and multiply during the GaN lateral growth, substantial shear stress must be present in the growth island. A recent in-situ stress measurement [8] revealed that GaN grows under a constant tensile stress on a sapphire substrate by MOVPE at 1050°C. The tensile stress (0.2 to 0.6 GPa depending on growth conditions) is not relaxed by thermal cycling to room temperature or annealing at the growth temperature. If a growth island is bonded to a highly tensile substrate, a high shear stress is expected adjacent to the film edge [9]. If this shear stress resolved on the slip plane is higher than the critical stress needed for slip, then dislocation glide can be invoked to relax the stress. As the island grows vertically and laterally, the expanding materials boundary and geometry effect may necessitate the generation of arrays of dislocations and the onset of c-axis tilting. Since the generation and interaction of dislocations in a stressed crystal with moving boundaries are too complicated to simulate, we have set out to simulate just the static stress distribution in the triangular ridge structure at the growth temperature.

A periodic extension of an 8- $\mu\text{m}$ -wide unit cell with a 3- $\mu\text{m}$ -wide growth window at the center is used for the stress simulations. As the temperature rises from room temperature to 1050°C, a uniform horizontal expansion of the unit cell is imposed beyond thermal expansion so that the GaN seed layer is under a tensile stress at the growth temperature. Added on top of the uniform growth stress are local tensile stress fields due to the smaller thermal expansion of the oxide mask layer relative to GaN. Fig. 4 shows the simulated distribution of  $\sigma_{xx}$ ,  $\sigma_{zz}$ , and  $\sigma_{xz}$  stresses in the 66° ridge structure at 1050°C. Here the x-axis is in the horizontal [1120] direction and the z-axis is in the vertical [0001] direction. The uniform growth stress  $\sigma_{xx}$  (set at 0.5 GPa) decreases rapidly to zero in the ridge island, and the thermal mismatch with the oxide mask layer contributes an extra 0.5 GPa in small regions at the window edges [Fig. 4(a)]. The vertical stress  $\sigma_{zz}$  and shear stress  $\sigma_{xz}$  close to the ridge surface [Fig. 4(b) and 4(c)] are linearly proportional to the GaN growth stress. Since the critical stress for dislocation glide, the Peierls stress, in a covalent crystal is typically 0.1% - 1% of the shear modulus and decreases with

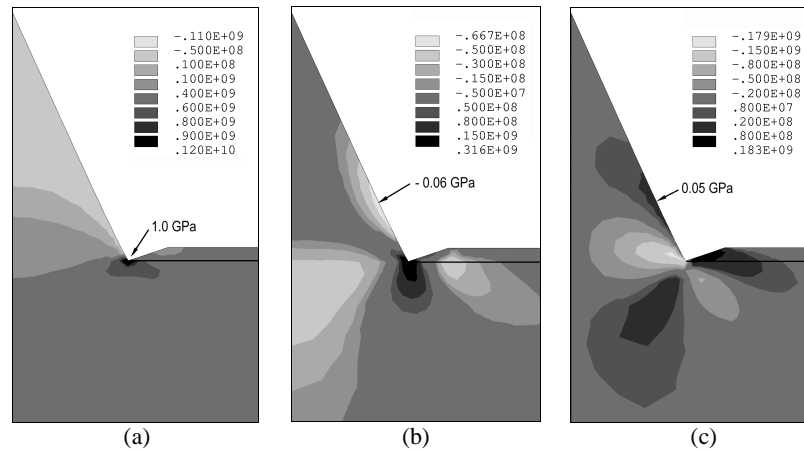


**Fig. 4** Stress distribution in the ridge structure at 1050°C prior to the onset of lateral growth: (a)  $\sigma_{xx}$  along the horizontal x-axis, (b)  $\sigma_{zz}$  along the vertical z-axis, and (c)  $\sigma_{xz}$  shear stress on the (0001) plane.

increasing temperature, our simulations suggest that 0.05 Pa shear stress should be high enough for dislocation motions at 1050°C.

It is noted that a high density of edge dislocations ( $> 2 \times 10^{10}/\text{cm}^2$ ) is generated locally in the high shear stress regions close to the mask edge, and dislocation pileups with Burgers vector  $b = 1/3[11\bar{2}0]$  are observed experimentally. From elasticity considerations, a dislocation with  $b = 1/3[11\bar{2}0]$  on the (0001) plane will be bent to the  $[1\bar{1}00]$  mask edge direction by the shear stress field. The observed pileups suggest that extensive stress relaxation is accomplished most likely via a Frank-Read type operation during the lateral growth.

## CONCLUSION

We have investigated the dislocation mechanisms involved in the lateral growth of GaN by HVPE on a patterned substrate. The lateral growth rate is highly sensitive to the growth temperature and is dependent on the exposed growth facets. The growth morphology changes drastically from a narrow ridge to a smooth and continuous film as the growth temperature increases from 1050 to 1100°C. Threading dislocations from the seed layer bend into laterally grown regions and multiply into arrays of edge dislocations lying parallel to the growth window. This multiplication and pileup of dislocations lead to a large-angle c-axis tilting in the laterally grown regions. Finite element stress simulations indicate that at a high growth temperature, the tensile growth stress in the GaN seed layer and the thermal stress from the mask layer both contribute to a high shear stress at the growth facets. The relaxation of this shear stress is believed to be the driving force behind the excessive dislocation activities and the c-axis tilting occurring during the lateral growth.

## ACKNOWLEDGMENT

This work was funded under the ONR MURI Grant #N00014-96-1-1179 through Dr. Colin Wood.

## REFERENCES

1. O. -H. Nam, M. D. Bremser, T. S. Zheleva, and R. F. Davis, *Appl. Phys. Lett.* **71**, 2638 (1997).
2. H. Marchand, X. H. Wu, J. P. Ibbetson, P. T. Fini, P. Kozodoy, S. Keller, J. S. Speck, S. P. DenBaars, and U. K. Mishra, *Appl. Phys. Lett.* **73**, 747 (1998).
3. A. Sakai, H. Sunakawa, and A. Usui, *Appl. Phys. Lett.* **71**, 2259 (1997).
4. A. Sakai, H. Sunakawa, and A. Usui, *Appl. Phys. Lett.* **73**, 481 (1998).
5. R. Zhang and T. F. Kuech, *Mat. Res. Soc. Symp. Proc.*, Vol. 512, 327 (1998).
6. W. Qian, M. Skowronski, M. De Graef, K. Doverspike, L. B. Rowland, and D. K. Gaskill, *Appl. Phys. Lett.* **66**, 1252 (1995).
7. F. C. Frank and W. T. Read, in *Symposium on Plastic Deformation of Crystalline Solids*, Carnegie Institute of Technology, 1950, p. 44.
8. S. Hearne, E. Chason, J. Han, J. A. Floro, J. Figiel, J. Hunter, H. Amano, and I. S. T. Tsong, *Appl. Phys. Lett.* **74**, 356 (1999).
9. M. Murakami, T. S. Kuan, and I. A. Blech, "Mechanical Properties of Thin Films on Substrates," in *Treatise on Materials Science and Technology*, Vol. 24, Academic Press, Inc., 1982, p.163-209.